HHS Public Access

Author manuscript

Knee. Author manuscript; available in PMC 2017 July 31.

Published in final edited form as:

Knee. 2015 October ; 22(5): 405–410. doi:10.1016/j.knee.2015.06.012.

MRI-based analysis of patellofemoral cartilage contact, thickness, and alignment in extension, and during moderate and deep flexion

Benjamin R. Freedman[1,2], **Frances T. Sheehan**[3], and **Amy L. Lerner**[1]

[1]Department of Biomedical Engineering, University of Rochester

[2]Department of Bioengineering, University of Pennsylvania

[3]Functional and Applied Biomechanics, National Institutes of Health

Abstract

Background—Several factors are believed to contribute to patellofemoral joint function throughout knee flexion including patellofemoral (PF) kinematics, contact, and bone morphology. However, data evaluating the PF joint in this highly flexed state have been limited. Therefore, the purpose of this study was to evaluate patellofemoral contact and alignment in low (0°), moderate (60°), and deep (140°) knee flexion, and then correlate these parameters to each other, as well as to femoral morphology.

Materials and Methods—Sagittal magnetic resonance images were acquired on 14 healthy female adult knees (RSRB approved) using a 1.5T scanner with the knee in full extension, mid-flexion, and deep flexion. The patellofemoral cartilage contact area, lateral contact displacement (LCD), cartilage thickness, and lateral patellar displacement (LPD) throughout flexion were defined. Intra- and inter-rater repeatability measures were determined. Correlations between patellofemoral contact parameters, alignment, and sulcus morphology were calculated.

Results—Measurement repeatability ICCs ranged from 0.94–0.99. Patellofemoral cartilage contact area and thickness, LCD, and LPD were statistically different throughout all levels of flexion ($p<0.001$). The cartilage contact area was correlated to LPD, cartilage thickness, sulcus angle, and epicondylar width ($r=0.47–0.72$, $p<0.05$).

Discussion—This study provides a comprehensive analysis of the patellofemoral joint throughout flexion throughout its range of motion.

Corresponding Author: Benjamin R. Freedman, B.S., University of Pennsylvania, 424 Stemmler Hall, 36th and Hamilton Walk, Philadelphia, PA, 19104-6081, USA, Tel: 413-537-3369, bfreed@seas.upenn.edu.

All authors contributed to the preparation of this manuscript.

Conflicts of Interest

The authors have no conflicts of interest to report.

Conclusions—This study agrees with past studies that investigated patellofemoral measures at a single flexion angle, and provides new insights into the relationship between patellofemoral contact and alignment at multiple flexion angles.

Keywords

Patellofemoral joint; Patellofemoral biomechanics; Knee; Deep knee flexion

Introduction

The patellofemoral (PF) joint is highly complex, undergoing six degree of freedom motion during knee extension and flexion. One of its primary functions is to act as a dynamic fulcrum transferring the force of the quadriceps to the tibia. Several mechanical factors are believed to contribute to this PF joint function throughout knee flexion, such as patellofemoral (PF) joint alignment [1–3], contact properties [4–6], and joint morphology [4, 7, 8]. Although many of these properties have been well studied during activities involving mid-flexion to terminal extension, studies involving deep knee flexion (knee flexion > 90°) have been understudied [9], and a comprehensive analysis describing the PF joint throughout flexion has been limited. Quantifying PF behavior in deep flexion is necessary to fully characterize the complete biomechanics of the PF joint.

Several studies have established that PF kinematics [10–12], alignment [1–3, 8, 10, 12–15], and contact [4–6, 12, 13, 15–21] vary from low to moderate knee flexion (0° – 60°). However, few studies have evaluated these parameters into deep knee flexion [10, 16]. Furthermore, no study to date has investigated the relationship between PF alignment and contact. An understanding of this relationship would help advance the clinical understanding of PF joint biomechanics, by either supporting or refuting the generally accepted causal links between PF kinematics/alignment, and PF joint contact. The various levels of knee flexion expose the patella to unique loading environments, thus it is crucial that these variables and their associations be evaluated across the range of knee flexion. Similar to terminal extension, in deep flexion, the femoral sulcus widens and provides less kinematic constraint on the patella [22]. However, unlike terminal extension, during deep flexion, the patella is suspended across the intercondylar notch [22] and the quadriceps' passive force is in its maximal range. Thus, understanding PF joint behavior requires a complete model that encompasses PF cartilage contact, joint alignment, and morphology at low, moderate, and deep knee flexion angles.

Therefore, the primary objective of this study was to evaluate the changes in PF cartilage contact area, thickness, centroid location, and PF joint alignment throughout the full range of knee flexion in pain-free subjects. The secondary objective was to determine whether the cartilage contact area was correlated with four variables (cartilage thickness, centroid location, PF joint alignment, and sulcus angle) throughout the full range of knee flexion. The relationship between the cartilage centroid location and lateral patellar displacement was also evaluated. We hypothesized that cartilage contact, thickness, and alignment would vary throughout flexion. Additionally, although relationships between PF contact parameters and alignment are assumed to exist [23], they have not been defined fully. Therefore, a

secondary hypothesis was that the lateral displacement of the contact centroid (LCD) would correlate to the lateral patellar displacement (LPD).

Methods and Materials

Study Design

Fourteen healthy female subjects (Age: 30.2 ± 9.3 years; Height: 158.3 ± 4.6 cm, Weight: 54.6 ± 7.7 kg), with no history of knee pain or surgery, were recruited for the study (Research Subjects Review Board (RSRB) approved). A single left knee was scanned for each subject. Sagittal T1-weighted images were acquired using a 1.5-Tesla magnetic resonance (MR) scanner (GE Signa Excite) with a 3D GRE sequence (FOV: 15cm, TE, 17ms; TR, 45ms; flip angle: 30°; slice thickness: 1–1.2 mm). For all knee flexion angles evaluated, the subject was positioned prone, and a custom knee positioning device (Figure 1) was used to align the knee in full extension (0°, FE), moderate flexion (60°, MF), and deep flexion (140°, DF) using a goniometer. Goniometer measurements were verified by measuring the knee flexion angle directly from the MR-images [24]. The subject was asked to relax their leg muscles, and the calf was lightly strapped in place to reduce motion artifact. Custom phased-array surface receiver coils were placed surrounding the knee, with a ring coil also placed on the posterior side for the full extension and moderate flexion positions [25]. Additionally, coronal images were acquired at the hip and ankle [26], as an assessment of tibiofemoral alignment, to measure the hip-knee-ankle angle (2D acute angle between the hip, knee, and ankle centers in the coronal plane).

PF Joint Contact and Alignment Measures

As was done previously [24, 27], all regions of interest (ROIs) were re-oriented to account for slight variations in subject placement within the MR scanner [28] across knee angles and across subjects using OsiriX (Pixmeo; Geneva, Switzerland). This process created a new orientation in which the femoral y-axis (f_y – the bisector of the femoral shaft in the mid-femoral sagittal image) was aligned with the vertical axis of the sagittal plane and the femoral x-axis (f_x – the posterior edge of the femur in the axial image containing the epicondylar line) was aligned with the horizontal axis in the axial plane.

All alignment measures were derived relative a coordinate system fixed within the femoral bone (Figure 2). The femoral origin (Fo) was defined as the deepest point in the sulcus at the axial level of the femoral epicondylar width. The patellar origin (PP) was defined as the most posterior point on the patella in the mid-patellar axial image. The lateral patellar displacement (LPD) was defined as the distance from Fo to PP in the femoral x-direction (Figure 2A–C) [2], with medial being positive. In addition, the sulcus angle [29] and epicondylar width were evaluated in the images acquired for terminal extension using previously reported methods [7].

The PF contact area, centroid location, and cartilage thickness were evaluated throughout flexion. For each sagittal image slice, the contact line between the patellar and femoral cartilage was identified in each image at each flexion angle (Figure 2D–F). The cartilage contact area was quantified by multiplying the sum of the length of each contact line by the

slice thickness [5]. The cartilage centroid (LCD) was defined by the image location containing the central region of contact. Its lateral location was defined relative to the Fo. The sum of the patellar and femoral cartilage thicknesses were determined by measuring the total distance between the patellar and femoral bone surfaces at the cartilage contact centroid, at an orientation perpendicular to the medial-lateral contact centroid (Figure 2D–F).

Due to the mode of contact in DF, the contact area and centroid was divided into medial and lateral components for all subjects (Figure 2C,F). The total contact area was defined as the sum of these components. To account for variation in subject size, the cartilage contact area, LPD, LCD, and thickness were scaled by the ratio of the subject to the current group average epicondylar width [30].

Statistical Analysis

Intra-rater reliability was evaluated for the PF alignment parameters (author BRF). Inter-rater reliability was evaluated for cartilage contact parameters (authors BRF and ALL). From these measures, intraclass coefficients (ICCs) were determined using a two-way mixed effects model for single measures (SPSS, IBM SPSS Inc. Version 20, Armonk, New York). In both cases, measurements were conducted blinded and the analysis began with the image set as acquired from the MR.

One-way repeated measures ANOVAs were used to determine if differences existed between flexion angles (FE, MF, DF) for the contact area and LPD. In addition, one-way repeated measures ANOVAs were used to determine if differences existed between flexion angles (FE, MF, DF-medial (M) side, and DF-lateral (L) side) for the cartilage thickness and LCD. Significant relationships ($p<0.05$) were further evaluated with one-tailed post-hoc paired T-tests and Bonferroni corrections. Pearson's correlation coefficients between LCD and LPD were calculated, and a paired T-test was used to determine if LCD and LPD were statistically different. In addition, correlation coefficients between PF contact area throughout flexion and thickness, LPD, sulcus angle, and epicondylar width were determined. A post hoc power analysis determined that the observed power was greater than 0.96 for all comparisons made that achieved statistical significance [31].

Results

MR-based measures showed that the knee achieved 60.2°±4.5° flexion in MF and 137.3° ±4.0° flexion in DF. With regard to tibiofemoral alignment, the mean HKA angle measured was 0.01°±1.86° [26]. Intra- and inter-rater measurement repeatability ICCs were excellent (Area: 0.94; LCD: 0.99, LPD: 0.94). A value of 0.90 is needed for "reasonable clinical validity" [30].

Flexion angle was a significant factor (Table 1, $p<0.001$) for PF cartilage contact area (Figure 3), thickness (Figure 4), lateral centroid displacement (LCD), and lateral patellar displacement (LPD). Post-hoc paired t-tests revealed that the cartilage contact area increased from FE to MF and DF, but was not different between MF and DF (Figure 3). In DF, the ratio of contact between the medial and lateral facets of patellar contact was 3.4:6.6 (Table

1). In addition, the cartilage thickness (Figure 4) in FE was less than MF ($p<0.001$). The cartilage thickness was higher for MF than for either facet (medial or lateral) in DF ($p<0.001$). The LPD was significantly more medial than the LCD at all knee flexion angles ($p<0.001$) (Table 1).

For relationships between PF cartilage contact and joint alignment, LPD was moderately correlated to LCD in FE and MF (r=0.57, 0.78, p= 0.02, 0.001), and was strongly correlated in DF (r=0.85, 0.96, p=0.001). Contact area was significantly correlated to LPD (r=0.72, p=0.002) in FE, cartilage thickness (r=0.57, p=0.02) in MF, the sulcus angle (r=0.47, p=0.04) in MF, and the epicondylar width in MF and DF (r=0.47, 0.48, p=0.04).

Discussion

This study provides a comprehensive analysis of the PF joint throughout flexion for single control cohort. As such, it provides much needed data on the state of the PF joint in deep flexion (DF), which is highly relevant to fully characterizing PF joint function into deep flexion. This improved understanding of the state of the PF joint throughout the knee's range of motion supports future developments in PF modeling and cadaveric joint simulators [32–37]. The direct evidence of a relationship between contact area and PF alignment, thickness, and morphological parameters will help support enhanced understanding of the PF joint biomechanics throughout knee flexion. The intra-rater measurement repeatability ICC for LPD (ICC=0.94) and inter-rater measurement repeatability ICCs for cartilage contact area (ICC=0.94) and LCD (ICC=0.99) were excellent. Together, these repeatability ICCs were above the value of 0.90 needed for "reasonable clinical validity" [30], which enables the study variables to be used in future research.

The contact area data were in agreement with past *in vivo* studies (Figure 5), but provide the first view into how this parameter varies *in vivo* throughout the entire range of motion for a single cohort. The majority of past studies focused on knee angles less than 60° demonstrated the same decrease in area from MF to FE as seen in the current study [4–6, 13, 17]. Nonlinearity may exist in early flexion [6], which was not observed in the current study, due to the fact that several knee angles in early to moderate flexion were not evaluated and that quadriceps activity was absent. Results in DF were similar to measurements by Nakagawa and colleagues [16]. The fact that contact area did not continue to increase from MF to DF indicates that during an exercise such as deep squats, the stress would rise as the required force in the quadriceps rises.

Our identification of relationships between PF contact, alignment, and morphology throughout knee flexion angles is an improvement over previous studies that only investigated such parameters in isolation. The correlations with contact area indicate that contact area is influenced by different parameters depending upon the posture of the knee. At full extension, the patella is at its peak superior location relative to the femoral sulcus. As such, contact area was related only to PF alignment (LPD) at this knee angle and the sulcus angle did not influence the contact area. In mid-flexion, the patella is well seated in the groove and contact area was influenced not by the PF alignment, but by the size and shape of the distal femur. Additionally, the relationship observed between the LPD and LCD

throughout knee flexion exemplifies the role that the sulcus plays in controlling PF alignment. Thus, pathological kinematics may arise when the influence of the sulcus is diminished by patella alta [38], patella baja, or altered femoral shape [7, 22]. It is likely that the behavior in deep flexion is much more complex than in FE and MF due to a combination of two separate contact points on the medial and lateral facets on the patella in addition to larger passive tissue constraints and quadriceps loading. For these reasons, the LPD and sulcus angle were not associated with contact area in DF. It is possible that the correlations between variables may increase if a cohort with PF pain or osteoarthritis was investigated due to increased variation in parameters [2, 24, 27]. Taken together, these relationships provide further evidence that the behavior of the PF joint is multifactorial and no individual property can adequately describe the contact patterns of the entire joint. This more expanded view of the potential causes of changes to contact area suggests that the source of pain likely varies both across subjects and knee angles for a single subject.

The primary limitation of the study was that measurements were made while subjects were non-weightbearing with muscles in a relaxed state. Thus, the dynamic effects of combined axial, torsional, and shear forces on the PF joint could not be examined. However, it has been demonstrated that weightbearing or quadriceps contracture increases cartilage contact area by 24% in low and moderate flexion [5], and 18% in deep flexion [16], respectively. Therefore, we believe our results are valid throughout flexion and will only vary by a simple scale factor if the joints are loaded. Joint loading may also affect patellar orientation. Previous studies have demonstrated that static unloaded joint positions partially predict dynamic patellar kinematics in the sagittal, transverse, and coronal planes [39, 40]. Of the knee flexion angles assessed, the effect of quadriceps contracture on PF joint orientation is likely greatest in low knee flexion, where the effects of the femoral sulcus are minimized and patellar maltracking is evident. Another potential limitation was that the correlations between contact, alignment, and morphological parameters do not imply causality. Future work will expand this protocol to study individuals with PFPS and subjects of both genders, but alterations to the methodology are likely needed to make it more tolerable for individuals with pain. Although the PF joint contains six degrees of freedom, only axial-plane kinematics was evaluated. Future studies will measure PF superior/inferior shift [37], anterior/posterior shift, flexion, tilt, and spin [11]. In addition, the PF contact thickness and centroid were only computed at the contact centroid. This centroid may not be indicative of the region of maximum stress, thus future work evaluating the causative relationships between the point of maximum PF joint stress versus the center of the contact area and its relationship to joint pain is needed. Future work is also necessary to compare the behavior of the joint across ethnicities [26, 41], as well as in knees that may be deficient in stability [42].

Conclusions

In conclusion, this study provides a comprehensive analysis of the PF joint throughout flexion in a consistent subject population. In doing so, this work is consistent with past studies that investigated PF measures in isolation, and provides new insights into the relationship between PF contact and alignment throughout flexion. This work, along with our previous study [43], have demonstrated the feasibility of using standard clinical MR-scanners to image the knee joint in deep flexion. A key feature was that subjects were

positioned prone while the torso was lifted to reduce the potential for geometric distortion within the imaging field [44], while allowing a wide range of knee flexion angles to be evaluated. This method may become even more feasible by using wide bore scanners, particularly for larger subjects. Continued work is necessary to similarly describe the complete behavior of the PF joint in individuals with PF pain.

Acknowledgments

This study was supported by DePuy Orthopaedics and the NSF GRFP. We are grateful for the technical contributions of Art Salo and Kristen Hovinga during image acquisition. Dr. Sheehan's contribution to this study was supported by the Intramural Research Program of the NIH.

References

1. Wilson NA, Press JM, Koh JL, Hendrix RW, Zhang LQ. In vivo noninvasive evaluation of abnormal patellar tracking during squatting in patients with patellofemoral pain. J Bone Joint Surg Am. 2009; 91:558–566. [PubMed: 19255215]
2. Sheehan FT, Derasari A, Fine KM, Brindle TJ, Alter KE. Q-angle and J-sign: indicative of maltracking subgroups in patellofemoral pain. Clin Orthop Relat Res. 2009; 468:266–275. [PubMed: 19430854]
3. MacIntyre NJ, Hill NA, Fellows RA, Ellis RE, Wilson DR. Patellofemoral joint kinematics in individuals with and without patellofemoral pain syndrome. J Bone Joint Surg Am. 2006; 88:2596–2605. [PubMed: 17142409]
4. Connolly KD, Ronsky JL, Westover LM, Kupper JC, Frayne R. Differences in patellofemoral contact mechanics associated with patellofemoral pain syndrome. J Biomech. 2009; 42:2802–2807. [PubMed: 19889417]
5. Besier TF, Draper CE, Gold GE, Beaupre GS, Delp SL. Patellofemoral joint contact area increases with knee flexion and weight-bearing. J Orthop Res. 2005; 23:345–350. [PubMed: 15734247]
6. Borotikar BS, Sheehan FT. In vivo patellofemoral contact mechanics during active extension using a novel dynamic MRI-based methodology. Osteoarthritis Cartilage. 2013; 21:1886–1894. [PubMed: 24012620]
7. Harbaugh CM, Wilson NA, Sheehan FT. Correlating femoral shape with patellar kinematics in patients with patellofemoral pain. J Orthop Res. 2010; 28:865–872. [PubMed: 20108348]
8. Moro-oka T, Matsuda S, Miura H, Nagamine R, Urabe K, Kawano T, Higaki H, Iwamoto Y. Patellar tracking and patellofemoral geometry in deep knee flexion. Clin Orthop Relat Res. 2002:161–168.
9. Kujala UM, Jaakkola LH, Koskinen SK, Taimela S, Hurme M, Nelimarkka O. Scoring of patellofemoral disorders, Arthroscopy. 1993; 9:159–163.
10. Hamai S, Dunbar NJ, Moro-oka TA, Miura H, Iwamoto Y, Banks SA. Physiological sagittal plane patellar kinematics during dynamic deep knee flexion, Int Orthop. 2013; 37:1477–1482.
11. Sheehan FT, Drace JE. Quantitative MR measures of three-dimensional patellar kinematics as a research and diagnostic tool. Med Sci Sports Exerc. 1999; 31:1399–1405. [PubMed: 10527311]
12. Kobayashi K, Hosseini A, Sakamoto M, Qi W, Rubash HE, Li G. In vivo kinematics of the extensor mechanism of the knee during deep flexion. J Biomech Eng. 2013; 135:81002. [PubMed: 23719832]
13. Hinterwimmer S, von Eisenhart-Rothe R, Siebert M, Welsch F, Vogl T, Graichen H. Patella kinematics and patello-femoral contact areas in patients with genu varum and mild osteoarthritis. Clin Biomech (Bristol, Avon). 2004; 19:704–710.
14. Narkbunnam R, Chareancholvanich K, Hanroongroj T. Sagittal plane evaluation of patellofemoral movement in patellofemoral pain patients with no evidence of maltracking, Knee Surg Sports Traumatol Arthrosc. 2013
15. Salsich GB, Perman WH. Patellofemoral joint contact area is influenced by tibiofemoral rotation alignment in individuals who have patellofemoral pain. J Orthop Sports Phys Ther. 2007; 37:521–528. [PubMed: 17939611]

16. Nakagawa S, Kadoya Y, Kobayashi A, Tatsumi I, Nishida N, Yamano Y. Kinematics of the patella in deep flexion. Analysis with magnetic resonance imaging. J Bone Joint Surg Am. 2003; 85-A: 1238–1242. [PubMed: 12851348]
17. Salsich GB, Ward SR, Terk MR, Powers CM. In vivo assessment of patellofemoral joint contact area in individuals who are pain free. Clin Orthop Relat Res. 2003:277–284. [PubMed: 14646727]
18. Farrokhi S, Keyak JH, Powers CM. Individuals with patellofemoral pain exhibit greater patellofemoral joint stress: a finite element analysis study. Osteoarthritis Cartilage. 2011; 19:287–294. [PubMed: 21172445]
19. Goudakos IG, Konig C, Schottle PB, Taylor WR, Singh NB, Roberts I, Streitparth F, Duda GN, Heller MO. Stair climbing results in more challenging patellofemoral contact mechanics and kinematics than walking at early knee flexion under physiological-like quadriceps loading. J Biomech. 2009; 42:2590–2596. [PubMed: 19656517]
20. Suzuki T, Hosseini A, Li JS, Gill TJt, Li G. In vivo patellar tracking and patellofemoral cartilage contacts during dynamic stair ascending. J Biomech. 2012; 45:2432–2437. [PubMed: 22840488]
21. Draper CE, Besier TF, Gold GE, Fredericson M, Fiene A, Beaupre GS, Delp SL. Is cartilage thickness different in young subjects with and without patellofemoral pain? Osteoarthritis Cartilage. 2006; 14:931–937. [PubMed: 16647278]
22. Amis AA. Current concepts on anatomy and biomechanics of patellar stability. Sports Med Arthrosc. 2007; 15:48–56. [PubMed: 17505317]
23. Powers CM, Bolgla LA, Callaghan MJ, Collins N, Sheehan FT. Patellofemoral pain: proximal, distal, and local factors, 2nd International Research Retreat. J Orthop Sports Phys Ther. 2012; 42:A1–54.
24. Freedman BR, Sheehan FT. Predicting three-dimensional patellofemoral kinematics from static imaging-based alignment measures. J Orthop Res. 2013; 31:441–447. [PubMed: 23097251]
25. Kwok WE, Zhong J, You Z, Seo G, Totterman SM. A four-element phased array coil for high resolution and parallel MR imaging of the knee. Magn Reson Imaging. 2003; 21:961–967. [PubMed: 14684197]
26. Hovinga KR, Lerner AL. Anatomic variations between Japanese and Caucasian populations in the healthy young adult knee joint. J Orthop Res. 2009; 27:1191–1196. [PubMed: 19242980]
27. Freedman BR, Brindle TJ, Sheehan FT. Re-evaluating the functional implications of the Q-angle and its relationship to in-vivo patellofemoral kinematics. Clinical Biomechanics. 2014
28. Shibanuma N, Sheehan FT, Stanhope SJ. Limb positioning is critical for defining patellofemoral alignment and femoral shape. Clin Orthop Relat Res. 2005:198–206. [PubMed: 15864053]
29. Aglietti P, Insall JN, Cerulli G. Patellar pain and incongruence. I: Measurements of incongruence. Clin Orthop Relat Res. 1983:217–224.
30. Sheehan FT, Derasari A, Fine KM, Brindle TJ, Alter KE. Q-angle and J-sign: indicative of maltracking subgroups in patellofemoral pain. Clin Orthop Relat Res. 468:266–275.
31. Faul F, Erdfelder E, Buchner A, Lang AG. Statistical power analyses using G*Power 3.1: Tests for correlation and regression analyses. Behavior Research Methods. 2009; 41:1149–1160. [PubMed: 19897823]
32. Elias JJ, Kilambi S, Cosgarea AJ. Computational assessment of the influence of vastus medialis obliquus function on patellofemoral pressures: model evaluation. J Biomech. 2010; 43:612–617. [PubMed: 20060526]
33. Elias JJ, Saranathan A. Discrete element analysis for characterizing the patellofemoral pressure distribution: model evaluation. J Biomech Eng. 2013; 135:81011. [PubMed: 23719962]
34. Fitzpatrick CK, Baldwin MA, Clary CW, Wright A, Laz PJ, Rullkoetter PJ. Identifying alignment parameters affecting implanted patellofemoral mechanics. J Orthop Res. 2012; 30:1167–1175. [PubMed: 22570224]
35. Fitzpatrick CK, Baldwin MA, Laz PJ, FitzPatrick DP, Lerner AL, Rullkoetter PJ. Development of a statistical shape model of the patellofemoral joint for investigating relationships between shape and function. J Biomech. 2011; 44:2446–2452. [PubMed: 21803359]
36. Baldwin MA, Clary C, Maletsky LP, Rullkoetter PJ. Verification of predicted specimen-specific natural and implanted patellofemoral kinematics during simulated deep knee bend. J Biomech. 2009; 42:2341–2348. [PubMed: 19720376]

37. Luyckx T, Didden K, Vandenneucker H, Labey L, Innocenti B, Bellemans J. Is there a biomechanical explanation for anterior knee pain in patients with patella alta?: influence of patellar height on patellofemoral contact force, contact area and contact pressure. J Bone Joint Surg Br. 2009; 91:344–350. [PubMed: 19258610]

38. Sheehan FT, Derasari A, Brindle TJ, Alter KE. Understanding patellofemoral pain with maltracking in the presence of joint laxity: complete 3D in vivo patellofemoral and tibiofemoral kinematics. J Orthop Res. 2009; 27:561–570. [PubMed: 19009601]

39. Freedman B, Sheehan FT. Predicting Three Dimensional Patellofemoral Kinematics from Static Imaging-Based Alignment Measures. Journal of Orthopaedic Research. 2012

40. Brossmann J, Muhle C, Schroder C, Melchert UH, Bull CC, Spielmann RP, Heller M. Patellar tracking patterns during active and passive knee extension: evaluation with motion-triggered cine MR imaging. Radiology. 1993; 187:205–212. [PubMed: 8451415]

41. Leszko F, Hovinga KR, Lerner AL, Komistek RD, Mahfouz MR. In vivo normal knee kinematics: is ethnicity or gender an influencing factor? Clin Orthop Relat Res. 2011; 469:95–106. [PubMed: 20814773]

42. Yao J, Snibbe J, Maloney M, Lerner AL. Stresses and strains in the medial meniscus of an ACL deficient knee under anterior loading: a finite element analysis with image-based experimental validation. J Biomech Eng. 2006; 128:135–141. [PubMed: 16532627]

43. Yao J, Lancianese SL, Hovinga KR, Lee J, Lerner AL. Magnetic resonance image analysis of meniscal translation and tibio-menisco-femoral contact in deep knee flexion. J Orthop Res. 2008; 26:673–684. [PubMed: 18183628]

44. Wang D, Strugnell W, Cowin G, Doddrell DM, Slaughter R. Geometric distortion in clinical MRI systems Part I: evaluation using a 3D phantom. Magn Reson Imaging. 2004; 22:1211–1221. [PubMed: 15607092]

Highlights

- Patellofemoral contact and alignment vary and correlate through deep knee flexion.
- Patellofemoral contact correlates to femoral shape in moderate and deep flexion.
- Standard clinical MR-scanners may be used to image the knee joint in deep flexion.

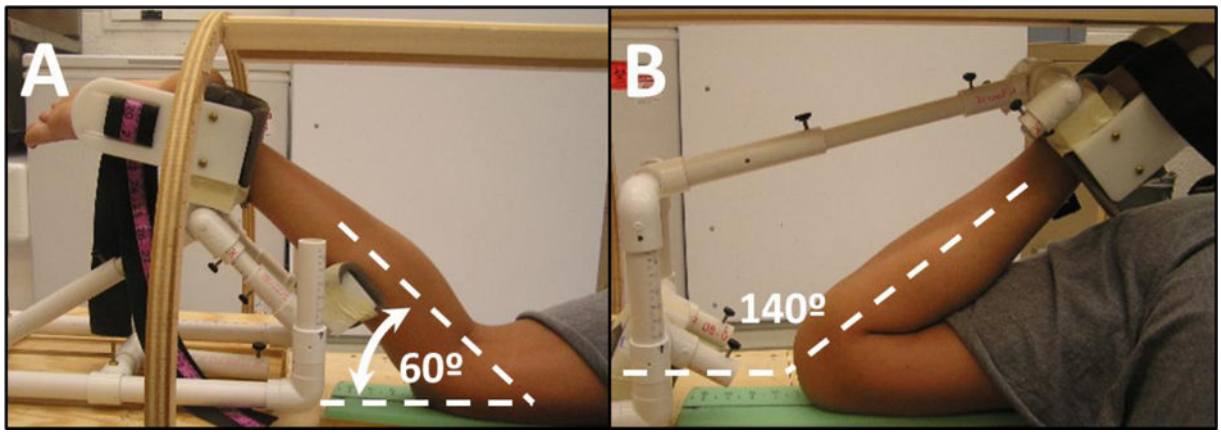

Figure 1. MR compatible knee positioning device

Knee positioning during MRI at (a) moderate flexion (60°) and (b) deep flexion (140°). Subjects were positioned prone. Phased array receiver coils (not shown) were placed around the knee to enhance image quality.

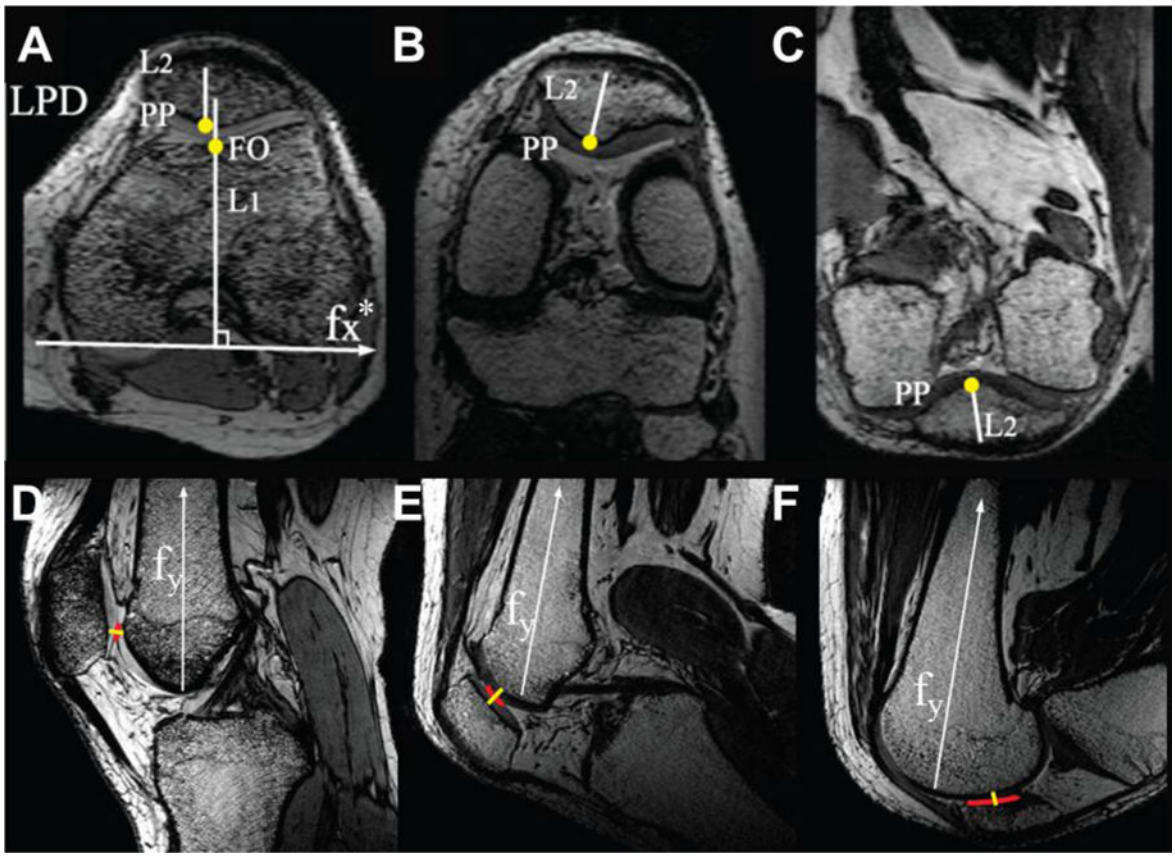

Figure 2. PF Joint Alignment and Contact Measures

(A–C) MR-based measures of lateral patellar displacement (LPD). LPD was defined as the medial/lateral distance between the posterior patella (PP) and the femoral origin/sulcus (FO) (i.e., between L_1 and L_2). The PP was defined as the most posterior patellar point in the mid-patellar image. The femur was rotated by the angle that the vectors f_x and f_y make with the magnet's left/right and superior/inferior axes, respectively, for each knee flexion angle evaluated. It is noted that f_y was measured on the sagittal image where the intercondylar notch on the posterior femur was greatest. F_x was defined from the axial image intersecting the intercondylar notch from this sagittal plane. Thus, f_x* denotes the propagated f_x to the mid-patellar plane, shown as an example in (A). (D–F) Method to determine contact area, centroid, and cartilage thickness. For each sagittal image slice, the contact region between the patellar and femoral cartilage was determined (red line) throughout flexion. Contact area was quantified by multiplying the contact region by the slice thickness. The cartilage centroid (LCD) was defined as the centroid of the contact area. The cartilage thickness was measured at the cartilage contact centroid (yellow line). A and D: FE (0° flexion); B and E: MF (60° flexion); C and F: DF (140° flexion).

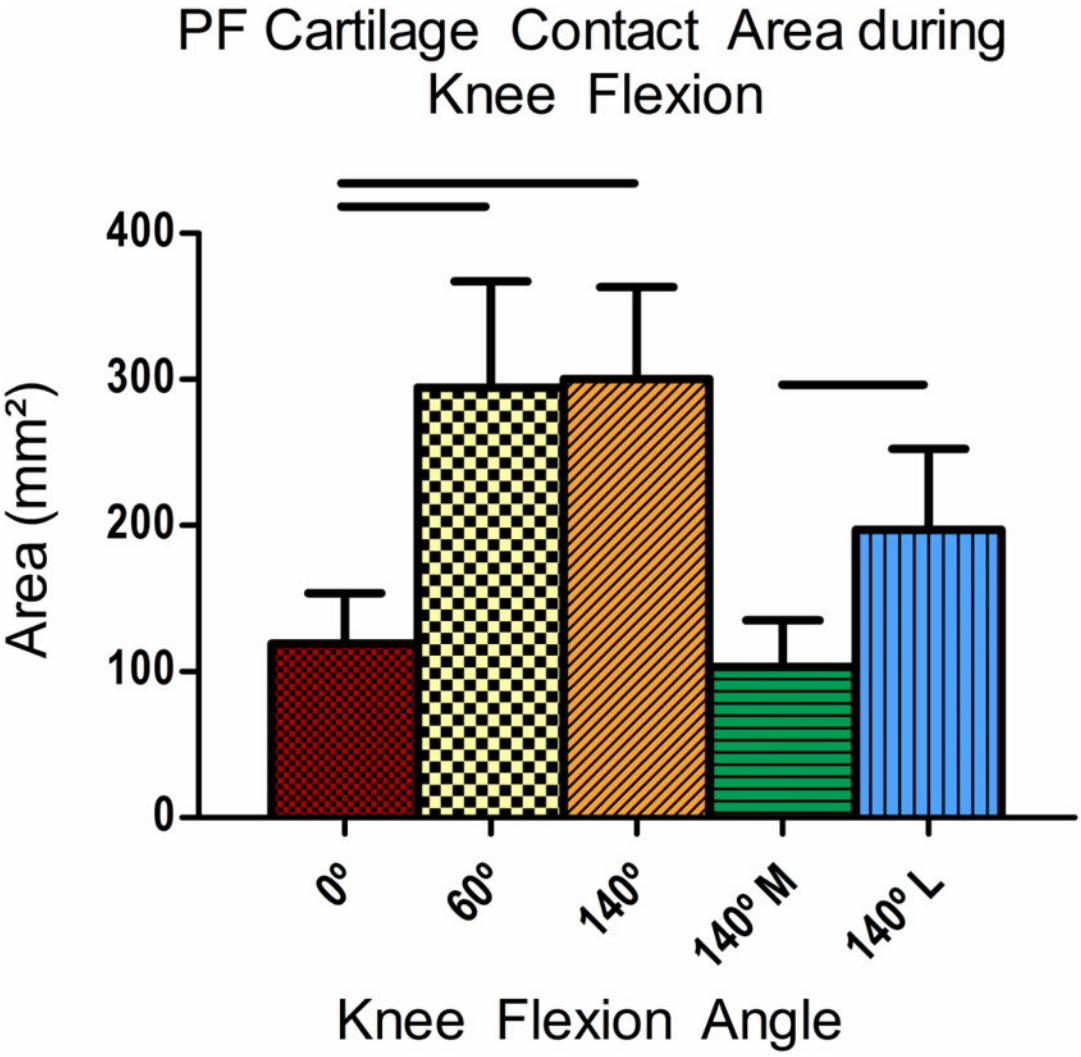

Figure 3. PF Cartilage contact area during knee flexion

As the knee was flexed, the PF cartilage contact area increased at 60° and 140°. In 140° of knee flexion, the contact area was divided into the medial (M) and lateral (L) facets of the patella contacting the femoral condyles. Solid lines indicate significant differences and error bars indicate standard deviation.

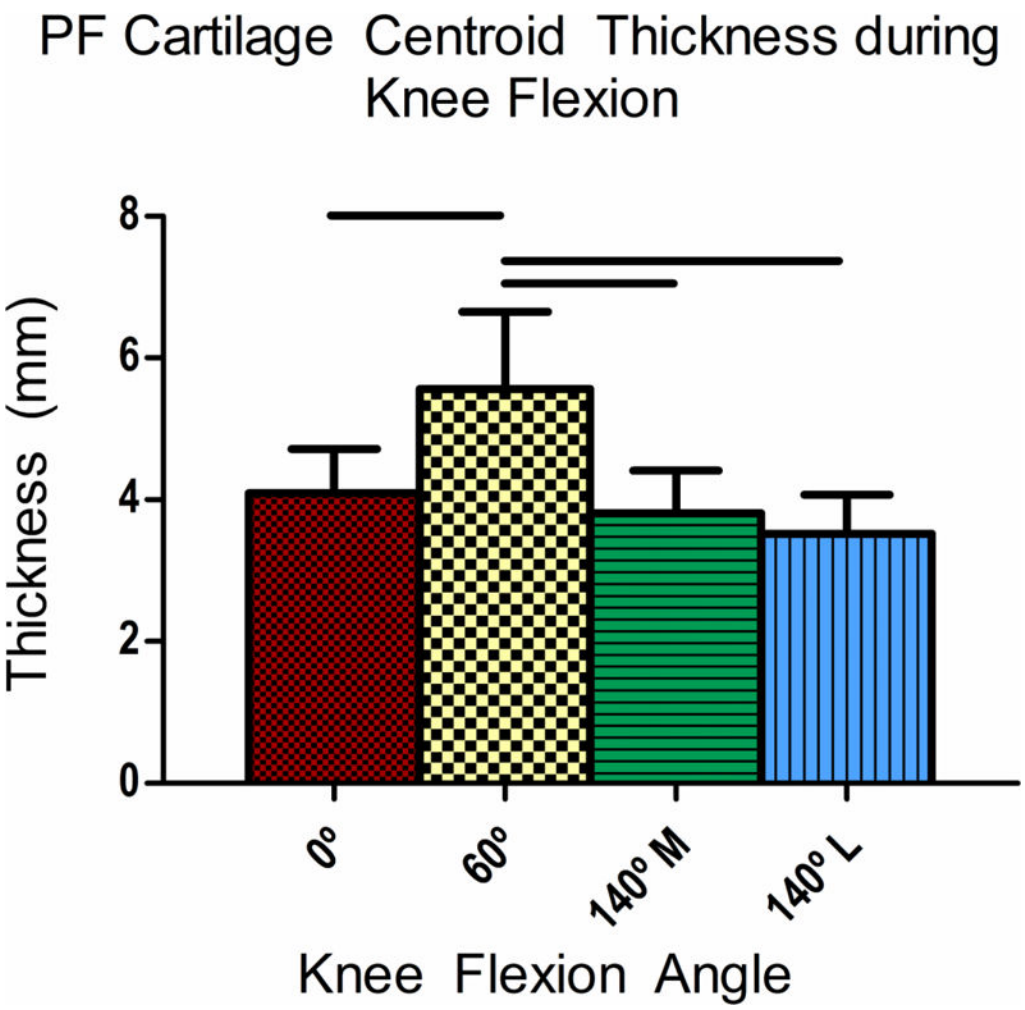

Figure 4. PF cartilage thickness at the contact centroid during knee flexion

The cartilage thickness was quantified from the sagittal image at the contact centroid. In 140° flexion, contact was divided between the medial (140°M) and lateral (140°L) patellar facets. As the knee was flexed from 0°, the cartilage thickness increased at 60°, but decreased in 140° flexion as measured for the lateral and medial patellar facets. Solid lines indicate significant differences and error bars indicate standard deviation.

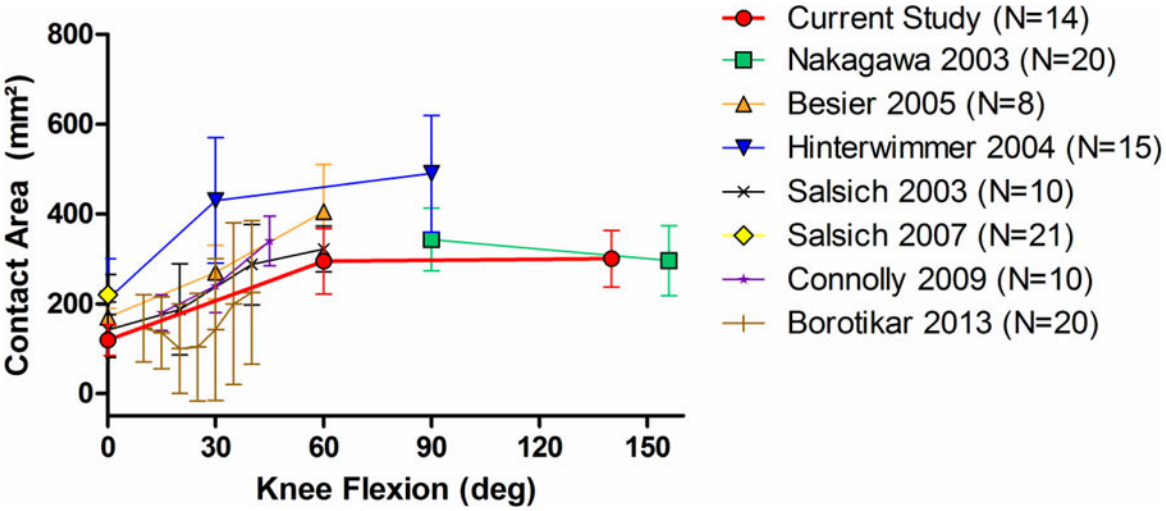

Figure 5. Summary of contact area throughout knee flexion with available literature

PF contact area increases from FE to MF and generally remains constant into deep flexion. Computed contact areas were similar to previous studies. Error bars indicate standard deviation.

Table 1

PF behavior through deep knee flexion

The cartilage contact area increased with knee flexion, whereas cartilage thickness was at a maximum at moderate flexion. The lateral contact displacement, although correlated to the lateral patellar displacement, was significantly more lateral. Finally, the cartilage contact area ratios demonstrated that the lateral facet of the patella occupied the most contact. FE = full extension, MF = moderate flexion, DF = deep flexion. M and L refer to the medial and lateral portions of contact when the knee is in deep flexion. LCD-lateral cartilage contact centroid displacement; LPD-lateral patellar displacement.

Parameter	FE (0°)	MF (60°)	DF (140°) Total	DF (140°) M	DF (140°) L
Cartilage Contact Area (mm^2)	119.0 ± 34.7	294.5 ± 72.8	300.4 ± 62.8	103.2 ± 31.9	197.2 ± 55.2
LCD (mm)	−7.9 ± 3.0	−7.3 ± 3.9	−8.8 ± 4.9	8.1 ± 4.2	−16.9 ± 4.4
LPD (mm)	1.6 ± 3.1	0.9 ± 1.3	−4.4 ± 4.4		
Cartilage Thickness (mm)	4.1 ± 0.6	5.6 ± 1.1		3.8 ± 0.6	3.5 ± 0.6
ML:Total Contact Ratios				3.4:10	6.6:10

Knee. Author manuscript; available in PMC 2017 July 31.

Table 2

Summary of previous work in the field

The current study demonstrates advancement over past works that did not investigate relationships between PF contact, alignment, and morphology throughout knee flexion. F= female, M= male, H=healthy, PFPS = patellofemoral pain syndrome, GV = genus varum, OA = osteoarthritis.

Publication	Sample Size & Demographic	Imaging Modality	Load bearing or Quads Activity	Full extension	Moderate Flexion	Deep Flexion	Contact Area	Contact Thickness/strain	Patellar/Femoral Shape	PF alignment	Measure Reliability	Reference
Current Study	F=14	MRI		x	x	x	x	x	x	x	x	
Narkbunnam 2013	H=40 PFPS= 30	Xray	x	x	x	x				x		[14]
Hamai 2013	H=9	Xray	x	x	x	x				x		[10]
Kobayashi 2013	H=7	Biplane Xray and Model	x	x	x	x	x	x				[12]
Borotikar 2013	F=20	MRI + Models	x	x	x		x	x				[6]
Freedman 2012	H=26 PFPS= 26	MRI		x	x					x	x	[27]
Farrokhi 2010	H=10, PFPS= 10	MRI	x	x				x				[18]
Wilson 2009	H=10 PFPS= 9	Optoelectronic motion capture		x	x					x		[1]
Connolly 2009	H=10 PFPS = 10	MRI		x	x		x	x	x			[4]
Salsich 2007	H=21 PFPS = 21	MRI				x	x			x		[15]
Draper 2006	H=16 PFPS= 34	MRI		x	x			x				[21]
Besier 2005	F=8 M=8	MRI	x	x	x		x					[5]
Hinterwimmer 2004	GV/OA=15 H=15	MRI	x	x	x		x			x		[13]
Salsich 2003	H=10	MRI	x	x	x		x					[17]
Nakagawa 2003	H=20	MRI	x		x	x	x					[16]
Morooka 2002	H=15	MRI		x	x	x			x	x		[8]